Vol 17 No 12, December 2008
1674-1056/2008/17(12)/4585-07

Chinese Physics B

© 2008 Chin. Phys. Soc.
and IOP Publishing Ltd

Synthesis and photoluminescence property of boron carbide nanowires*

Bao Li-Hong(鲍丽宏), Li Chen(李 晨), Tian Yuan(田 园), Tian Ji-Fa(田继发), Hui Chao(惠 超), Wang Xing-Jun (王兴军), Shen Cheng-Min (申承民), and Gao Hong-Jun(高鸿钧)†

Beijing National Laboratory for Condensed Matter Physics, Institute of Physics, Chinese Academy of Sciences, Beijing 100190, *China*

(Received 19 June 2008; revised manuscript received 24 June 2008)

Large scale, high density boron carbide nanowires have been synthesized by using an improved carbothermal reduction method with $B/B_2O_3/C$ powder precursors under an argon flow at 1100°C. The boron carbide nanowires are 5–10 μm in length and 80–100 nm in diameter. Transmission electron microscopy (TEM) and selected area electron diffraction (SAED) characterizations show that the boron carbide nanowire has a B_4C rhombohedral structure with good crystallization. The Raman spectrum of the as-grown boron carbide nanowires is consistent with that of a B_4C structure consisting of $B_{11}C$ icosahedra and C-B-C chains. The room temperature photoluminescence spectrum of the boron carbide nanowires exhibits a visible range of emission centred at 638 nm.

Keywords: carbothermal reduction, vapour–liquid–solid (VLS), Raman, photoluminescence
PACC: 6146, 9260, 7855, 7830G

1. Introduction

Since the discovery of carbon nanotubes by Iijima[1] in 1991, one-dimensional lightweight semiconducting nanostructures,[2−5] have aroused the great interest due to their special structures and electronic properties. Among these lightweight semiconductors boron carbide is an important material due to its unique properties and potentially widespread applications. It has a low density (2.5 gcm^{-3}), high melting point (> 2400°C), high strength and Young's modulus, and high-temperature thermal properties.[6−8] It is the third hardest material coming after the diamond and cubic boron nitride, but with very high temperature stability. It has a high neutron capture-section.[9] It has wide applications especially under extreme conditions, such as ceramic armours, neutron absorbers in the nuclear industry, and a potential material for high-temperature energy conversion.[6−10] In the past years, much effort has been devoted to the synthesis of boron carbide nanostructures. Methods of preparation include carbothermal reduction of boron oxides,[11−15] chemical vapour deposition (CVD) and plasma enhanced CVD (PECVD),[16−19] carbon nanotube (CNT) template assisted growth,[19−22] a porous alumina temple technique,[23] electrostatic pinning[24] and thermal evaporation of B_4C powder.[25] Zhang *et al*,[16] Mcllroy *et al*[17] have grown boron carbide nanowires, nanonecklaces and nanosprings through the PECVD method. Aligned boron carbide nanofibres have been fabricated by using a porous alumina template method. In addition, pure polycrystalline or crystalline, pure boron carbide nanowires[22] or encapsulates of boron carbide nanowires into BN or boron carbonitride (BCN) nanotubes[21] have been synthesized by using a CNT template method. Xue and Bando[11] and Ma and Bando[12,13] performed a specific investigation on the growth of boron carbide nanowires via a carbothermal vapour–liquid–solid (VLS) growth mechanism starting with $C/B/B_2O_3$ powder precursors with or without Fe catalyst. However, the growth of boron carbide nanowires requires a higher temperature (above 1600°C). Therefore, controllable growth of boron carbide nanowires with high density, single phase, mono-morphology and uniform size distributions becomes a key issue for technological applications.

*Project supported by the National High Technology Development Program of China (Grant No 2007AA03Z305), the state Key Development Program for Basic Research of China (Grant No 2007CB935503), the National Science Foundation of China (Grants Nos 60571045, 60620120443 and Guo-JI He-Zuo).

†Corresponding author. E-mail: hjgao@aphy.iphy.ac.cn

In this paper, we present an improved carbothermal method to synthesize boron carbide nanowires with a mixture of boron powder and Fe_3O_4nanoparticles coated Si (111) wafer as substrate, where the synthesis temperature is successfully lowered to 1100°C. Detailed structural and compositional analysis indicate that the as-grown boron carbide nanowires have a B_4C rhombohedral ($R\bar{3}m$, No.166) structure.[26] The corresponding growth mechanism and chemical processes are also discussed. The Raman spectrum of the boron carbide nanowires confirms that the B_4C structure is composed of $B_{11}C$ icosahedra and C-B-C chains.[27−29] Photoluminescence emission properties of boron carbide nanowires are measured to explore the potential applications in future optical emitting devices.

2. Experimental

2.1. Preparation of Fe_3O_4 Nanoparticle

In past years, we have successfully fabricated a few kinds of nanoparticles.[30−33] Here we used Fe_3O_4 nanoparticles as a catalyst to fabricate boron carbide nanowires through a carbothermal reduction method. Fe_3O_4 nanoparticles with diameters of less than 10 nm were synthesized by high temperature solution phase reduction of iron (III) acetylacetonate, $Fe(acac)_3$, with 1, 2-hexadecanediol in the presence of oleic acid and oleylamine.[34,35]

2.2. Fabrication of Boron Carbide Nanowires

A horizontal tube furnace was used to synthesize one-dimensional boron carbide nanowires. Boron powder (99.9%), boron oxide powder (99.99%) and carbon powder (99.99%) with the molecular ratio 2:1:1 were ground together as precursors and loaded into an alumina boat. The Fe_3O_4 nanoparticles were first dropped onto the Si (111) wafer, and then a small amount of boron powder was immerged into the Fe_3O_4 liquid drops on the Si (111) wafer. The coated Si (111) wafer, which was used as a substrate, was placed above the alumina boat in the reaction region, and the boat was removed from the reaction region prior to the growth of boron carbide nanowires. The temperature and gas flow rate were controlled for the ideal nanowires growth. The boron carbide nanowires were grown by using a two–step increasing temperature method. First, when the temperature of the reaction region reached 400°C, the alumina boat was immediately transferred into the reaction region and kept there for 30 min to eliminate the remaining oleic acid and oleylamine of Fe_3O_4 nanoparticles. Second, the temperature of the reaction region was quickly increased to 1100°C at a rate of 10°C/min, during which the alumina boat was kept out of the reaction region. A gas flow of 300sccm high purity (99.99%) Ar gas was fed into the tube during the above two process. Once the temperature reached 1100 °C, the alumina boat was again transferred to the reaction region to initialize the growth of boron carbide nanowires. The reaction lasted for 2 h at a constant 30 sccm flow rate of high purity Ar gas. After the furnace cooled down to room temperature, dark brown or black product was obtained on the surface of the substrate.

2.3. Characterization of boron carbide nanowires

Field–emission type scanning electron microscopy (SEM) (XL–SFEG, FEI Corp) was used for morphological observation of boron carbide nanowires. Transmission electron microscopy (TEM) (Tecnai–20, PHILIPS Cop.) and high-resolution transmission electron microscopy (HRTEM) (Tecnai F20, FEI Corp.) with electron energy loss spectrometer (EELS) were employed to perform the microanalysis of boron carbide nanowires. Raman and photoluminescence (PL) measurements of boron carbide nanowires films were recorded with JY–HR800 spectrometer system with a charge coupled device (CCD) detector and an optical microscopic system ranging from 200 to 2000 cm^{-1} at room temperature. A 532 nm Nd–YAG laser with an output power of 3 mW was used for excitation.

3. Results and discussion

The SEM images reveal that a large number of nanowires have been grown on the surface of the silicon substrate as shown in Fig.1. These nanowires are very smooth on the surface and uniform along the whole length. They have diameters of 20–100 nm with a mean diameter of around 90 nm and lengths of 5–10μm. The nanowires are straight each with a spherical Fe_3O_4 nanoparticle on the tips of the nanowires, which implies that they grew through the VLS growth mechanism.[29] (Fig.1(c)) Figure 1(d) is a high resolution SEM image of a single nanowire. The bright spherical nanoparticle is just the alloy droplet of the

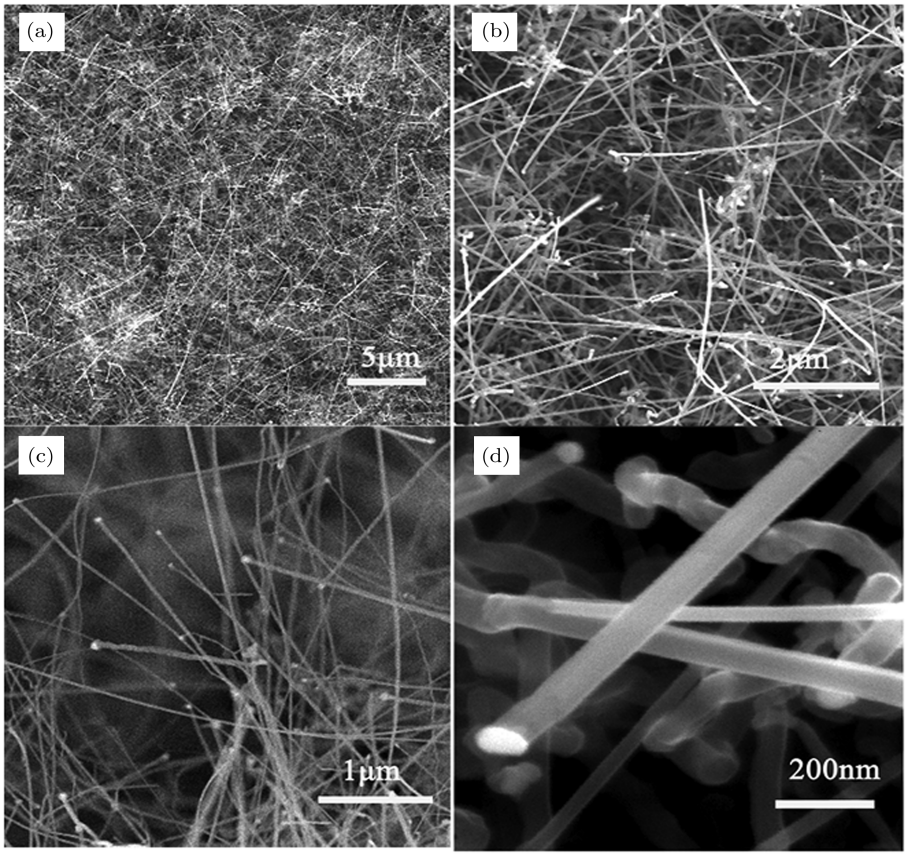


Fig.1. (a) and (b) Low magnification SEM images showing that the boron carbide nanowires with a large scale, high density and high aspect ratio are grown on the Si (111) substrate. (c) High magnification SEM image of the boron carbide nanowires, and the spherical tips of the nanowires are Fe_3O_4catalytic nanoparticles. (d) HRSEM image of a single boron carbide nanowire.

catalytic particle. Figure 2(a) shows a low magnification bright–field TEM image of a single nanowire. Selected area electron diffraction (SAED) was observed on different sections of the nanowire to determine its structure. All the SAED patterns are the same as shown in the inset of Fig.2(a), confirming that the as-grown nanowire is single crystalline. The calculated lattice constants are $a = 0.5600$ nm and $c = 0.1208$ nm, which agree well with the values of rhombohedral B_4C from the JCPDS database (35–0798).[26] Figure 2(b) shows a high–resolution TEM (HRTEM) image of a single boron carbide nanowire. The lattice resolved image further confirms the crystalline nature of the nanowire and the clearly resolved 0.40 nm distance between (003) plane is labelled. The preferential growth direction of the nanowire was determined to be the [003] direction (shown in Fig.2(b)). The outer thin amorphous layer is an oxide sheath, and formed when the crystalline boron carbide nanowire were exposed to air.

Chemical compositions of different parts of the nanowires were analysed by electron energy loss spectroscopy (EELS). Figure 3 depicts a typical EELS spectrum from the middle and the tip of the nanowire. Ionization edges around 188 and 284 eV are observable in the spectrum corresponding to the K–ionization edges of boron and carbon, respectively. No oxygen, iron or any other impurities could be detected from the middle of the nanowire as shown in Fig.3(a). This indicates that the nanowire is composed of B and C. Quantitative analysis of the EELS spectrum yields the elemental concentration of the nanowire. The C- to B- atomic ratio is calculated as 0.26 ± 0.036, close to B_4C (C/B $\approx$ 0.25). Except B and C, Fe and O were detected by EELS spectrum from the tip of the nanowire (Fig.3(b)). As shown in the inset of Fig.3(b), both oxygen (K–ionization edge at 532 eV) and iron (L–ionization edge at 708eV) were detected in the tip portion of the nanowire. This shows that the catalytic Fe_3O_4 nanoparticle only exists at the tip of the nanowire, which further confirms the VLS growth mechanism of the boron carbide nanowires.

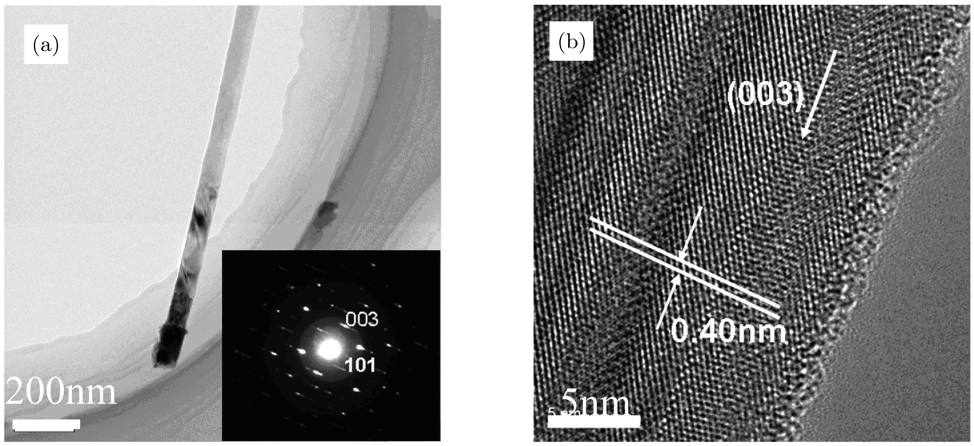


Fig.2. TEM and HRTEM images of the boron carbide nanowires. (a) TEM image of a single boron carbide nanowire, the SAED pattern (inset) confirms the crystalline nature of the nanowire. (b) The corresponding HRTEM image showing crystal structure and preferential growth along the [003] direction.

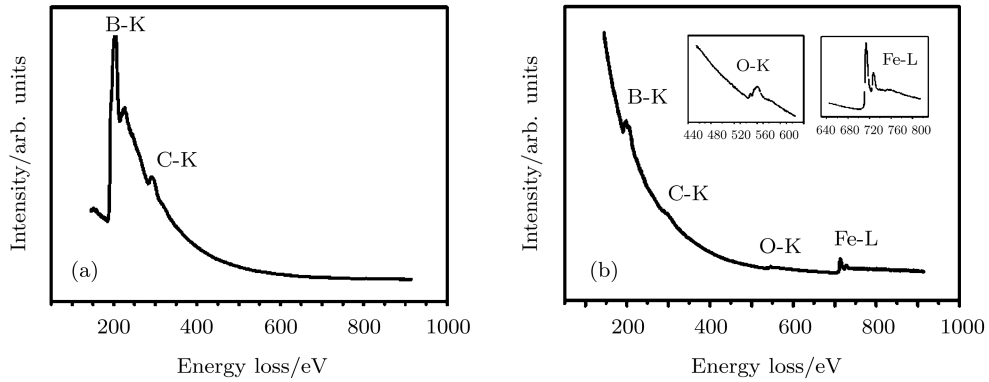


Fig.3. EELS spectra of the boron carbide nanowires. (a) A typical EELS spectrum in the middle of the nanowire shows that the nanowires are composed of B and C and B/C ratio is about 4:1. (b) A typical EELS spectrum from the spherical tip of the nanowire shows that the tip contains B, C, Fe and O.

The elemental mapping by energy filtered transmission electron microscopy (EFTEM) was used to further investigate the elemental distribution of the nanowires. Figure 4(a) is a zero–loss filtered image, and Figs.4(b)–4(d) shows elemental mappings of boron, carbon, and oxygen, respectively. The boron mapping, shown in Fig.4(b), demonstrates that the boron atoms distribute uniformly in the nanowire, and the brightest contrast confirms that boron is the main element. The carbon mapping (Fig.4(c)) shows that the carbon atoms also distribute uniformly in the nanowire, but due to the difference in contrast between the nanowire and the copper TEM grid, the brightness is not so clear. The oxygen mapping (Fig.4(d)) indicates that the oxygen atoms distribute mainly on the surface of the nanowire, and from the lattice-resolved TEM image (Fig.2(b)) we can see that the amorphous oxide layer is very thin (several Å). The EELS and TEM results suggest that the nanowires are B_4C nanowires with a very thin amorphous layer.

In our experiments, Fe_3O_4 nanoparticles were employed as a catalyst to fabricate boron carbide nanowires. We also tried to synthesize boron carbide nanowires without the Fe_3O_4 catalyst, but no 1D boron carbide nanomaterials were found on the surface of the Si (111) substrate. Moreover, the fact that iron was detected in the EELS spectrum only at the tips of the boron carbide nanowires suggests that the Fe_3O_4 catalyst play a key role in forming boron carbide nanowires, and the growth mechanism should be a VLS growth mechanism. Due to the high melting point of boron carbide (2400°C) materials, it was reported in the earlier work on the synthesis of boron carbide nanomaterials by using the carbothermal method that the synthesis temperature was in a

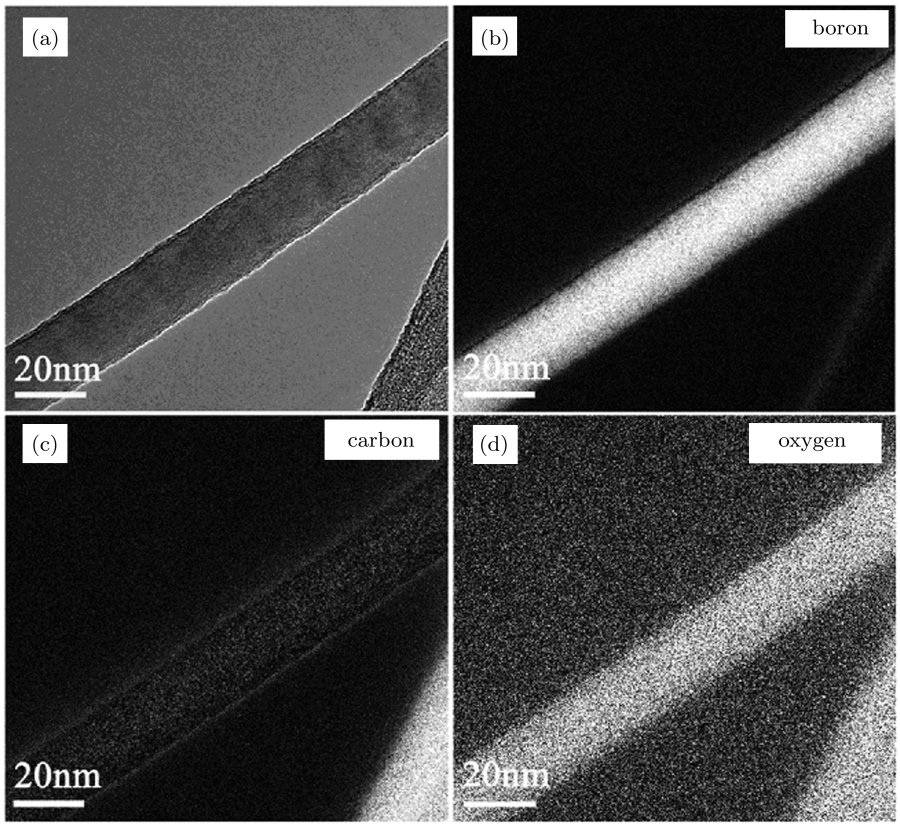


Fig.4. EFTEM images showing the elemental distribution of the nanowire, where panel (a) shows the zero-loss image indicating the morphology of the nanowire, and panels (b)–(d) display boron, carbon, oxygen mappings, respectively.

range of 1300–1700°C.[14−16] Here, using 10 nm Fe_3O_4 nanoparticles as a catalyst, the synthesis temperature successfully decreased down to 1100°C. The possible chemical reactions that took place can be written as

$$B_2O_3(s) \xrightarrow{400^\circ C} B_2O_3(l), \quad (1)$$

$$2B_2O_3(l) + 2B(s) \rightarrow 3B_2O_2(g), \quad (2)$$

$$2B_2O_3(l) + 7C(s) \rightarrow B_4C(s) + 6CO(g), \quad (3)$$

$$2B_2O_2(g) + 5C(s) \rightarrow B_4C(s) + 4CO(g), \quad (4)$$

$$2B_2O_3(l) + 8CO(g) \rightarrow B_4C(s) + 7CO_2(g), \quad (5)$$

$$2B_2O_2(g) + 6CO(g) \rightarrow B_4C(s) + 5CO_2(g). \quad (6)$$

At 1100°C, B_2O_3 in the alumina boat transformed from solid to liquid (Eq.(1)), and then reacted with solid boron in the alumina boat to form diametric boron dioxide (B_2O_2) vapour (Eq.(2)),[16] Meanwhile, Fe_3O_4 and boron alloy nanoclusters formed on the surface of Si (111) substrate, and they served as the energetically favoured sites for the condensation and precipitation for the reactant vapour. Then, the B_2O_2 vapour and B_2O_3 liquid reacted with C to form B_4C (Eqs.(3) and (4)), and the CO gas generated in the reactions further reacted with B_2O_2 and B_2O_3 to form B_4C solid (Eqs.(5) and (6)). The condensation and precipitation of B_4C took place on the Fe_3O_4 and boron nanoclusters. B_4C nanowires growth began when the B_4C species became supersaturated in the Fe_3O_4 and boron alloy nanoclusters.

A Raman spectrum is given in Fig.5(a) from excitation at 532 nm. From the figure the strong Raman peaks at 250, 320, 481, 534, 726 and 1086 cm^{-1} and two shoulders at 824 and 995 cm^{-1} are observed. The narrow band at 481 cm^{-1} is associated with the stretching mode of C-B-C chains and the peak at 534 cm^{-1} represents the vibrational mode of $B_{11}C$ icosahedra,[9,27,29,36] which is similar to that of bulk B_4C crystal. The A_{1g} modes at 726 and 1086 cm^{-1} are assigned to the breathing mode of the icosahedral $B_{11}C$ structure.[27,36,37] The broad band at about 250 cm^{-1} has no certain origin, and compared with the 270 cm^{-1} peak of the pristine B_4C,[27] which is attributed to the rotating mode of C-B-C chain and

wagging icosahedra structure, it shifts about 20 cm^{-1}. The broad band at around 320 cm^{-1} corresponds to the rotating C-B-B chain and wagging icosahedra structure.[36] All the Raman peaks are broadened compared with those of bulk B_4C[27,36,37] due to the finite size effect.[38]

Figure 5(b) shows the room temperature photoluminescence spectrum of B_4C nanowires thin film under 532 nm light excitation. The spectrum is composed of one broad band centred at 638 nm. Theoretical calculations and former experiments indicated that the photoluminescence energy of bulk B_4C was 1.563 (1.572) eV, which corresponds a wavelength of about 795 nm.[39−41] The photoluminescence peak of B_4C nanowires produced a blue–shift compared with that of bulk B_4C material, which might be due to the quantum confinement effect.[42,43] Vast *et al*[36] assigned the 795 nm peak to the direct or indirect band-band recombination of free excitons. We believe that the broad band arises from strong electron–phonon interactions or distributions of different energy levels of trap centres. The visible–light photoluminescence emission properties of as–grown B_4C nanowires illustrate their potential applications in visible optical emission devices.

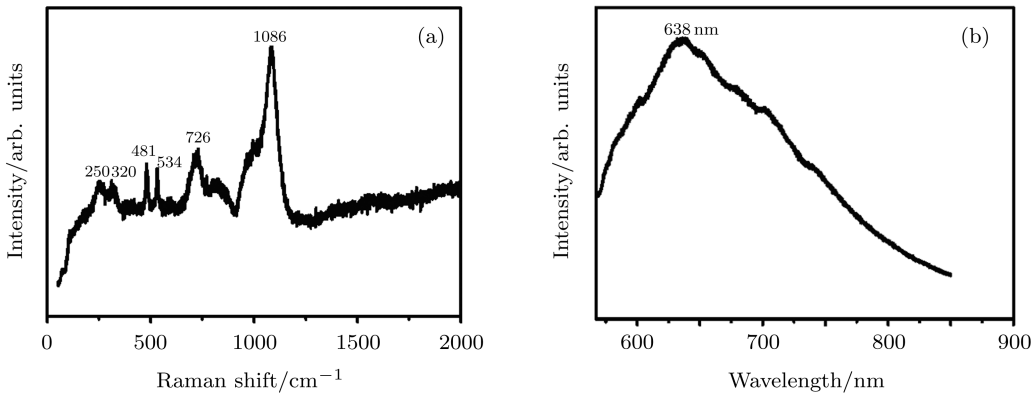


Fig.5. (a) Raman spectrum of the boron carbide nanowire thin film; (b) The room temperature photoluminescence spectrum of boron carbide nanowire thin film under 532 nm laser excitation.

4. Conclusions

Large scale, high density single crystalline boron carbide nanowires have been synthesized by using an improved carbothermal reduction method. The boron carbide nanowires have lengths of 5–10 μm and an average diameter of 90 nm. TEM and SAED results show that the boron carbide nanowire has a B_4C rhombohedral structure with good crystallization. The growth mechanism is a typical VLS mechanism. The Raman spectrum of the as-grown boron carbide nanowires is consistent with that of a B_4C structure made up of $B_{11}C$ icosahedra and C-B-C chains. The photoluminescence emission spectrum of the boron carbide nanowires exhibits a visible orange emission centred at 638 nm.

Acknowledgements

We thank the Centre for Biological Electron Microscopy, the Institute of Biophysics, Chinese Academy of Sciences for the help of TEM characterization.

References

[1] Iijima S 1991 *Nature* **354** 56
[2] Chopra N G, Luyken R J, Cherrey K, Crespi V H, Cohen M L, Louie S G and Zettl A 1995 *Science* **269** 966
[3] Stéphan O, Ajayan P M, Colliex C, Redlich P, Lambert J M, Bernier P and Lefin P 1994 *Science* **266** 1683
[4] Wang X J, Tian J F, Yang T Z, Bao L H, Hui, C, Liu F, Shen C M, Xu N S, Gu C Z and Gao H J 2007 *Adv. Mater.* **19** 4480
[5] Liu F, Cao P J, Zhang H R, Tian J F, Xiao C W, Shen C M, Li J Q and Gao H J 2005 *Adv. Mater.* **17** 1893
[6] Wood C and Emin D 1984 *Phys. Rev.* B **29** 4582
[7] Chen M W, McCauley J W and Hemker H J 2003 *Science* **299** 1563
[8] Sezer A O and Brand J I 2001 *Mater. Sci. Eng.* B **79** 191
[9] Lazzari R, Vast N, Besson J M, Baroni S and Dal Corso A 1999 *Phys. Rev. Lett.* **83** 3230

[10] Emin D and Aselage T L 2005 *J. Appl. Phys.* **97** 013529
[11] Xu F F and Bando Y 2004 *J. Phys. Chem.* B **108** 7651
[12] Ma R Z and Bando Y 2002 *Chem. Mater.* **14** 4403
[13] Ma R Z and Bando Y 2002 *Chem. Phys. Lett.* **364** 314
[14] Carlsson M, Garcia-Garcia F J and Johsson M J 2002 *Cryst. Growth* **236** 466
[15] Johnsson M 2004 *Solid State Ionics* **172** 365
[16] Zhang D, McIlroy D N, Geng Y and Norton M G 1999 *J. Mater. Sci. Lett.* **18** 349
[17] Mcllroy D N, Zhang D, Kranov Y and Norton M G 2001 *Appl. Phys. Lett.* **79** 1540
[18] Ma R Z, Bando Y, Sato T and Kurashima K 2001 *Chem. Phys. Lett.* **350** 434
[19] Dai H J, Wong E W, Lu Y Z, Fan S S and Lieber C M 1995 *Nature* **375** 769
[20] Han W, Bando Y, Kurashima K and Sato T 1999 *Chem. Phys. Lett.* **299** 368
[21] Han W, Kohler-Redlich P, Ernst F and Rohler M 1999 *Chem. Mater.* **11** 362
[22] Wei J Q, Jiang B, Li Y H, Xu C L, Wu D H and Wei B Q 2002 *J. Mater. Chem.* **12** 3121
[23] M J Pender and L G Sneddon 2000 *Chem. Mater.* **12** 280
[24] Welna D T, Bender J D, Wei X, Sneddon L G and Allcock H R 2005 *Adv. Mater.* **17** 859
[25] Zhang H Z, Wang R M, You L P, Yu Y, Chen H, Yu D P and Chen Y 2007 *New J. Phys.* **9** 13
[26] JCPDS-International Centre for Diffraction Data, PCPDFWIN, v.2.4, 2003
[27] Tallant D R, Aselage T L, Campbell A N and Emin D 1989 *Phys. Rev.* B **40** 5649
[28] Kuhlmann U and Werheit H 1994 *J. Alloys Compd.* **205** 87
[29] Aselage T L, Tallant D R and Emin D 1997 *Phys. Rev.* B **56** 3122
[30] He S T, Xie S S, Yao J N, Gao H J and Pang S J 2002 *Appl. Phys. Lett.* **81** 150
[31] He S T, Yao J N, Jiang P, Shi D X, Zhang H X, Xie S S, Pang S J and Gao H J 2001 *Langmuir* **17** 1571
[32] Yang H T, Shen C M, Wang Y G, Su Y K, Yang T Z and Gao H J 2004 *Nanotechnology* **15** 70
[33] Yang H T, Shen C M, Su Y K, Yang T Z, Gao H J and Wang Y G 2003 *Appl. Phys. Lett.* **82** 4729
[34] Yang T Z, Shen C M, Li Z A, Zhang H R, Xiao C W, Chen S T, Xu Z C, Shi D X, Li J Q and Gao H J 2005 *J. Phys. Chem.* B **109** 23233
[35] Xiao C W, Yang H T, Shen C M, Li Z A, Zhang H R, Liu F, Yang T Z, Chen S T and Gao H J 2005 *Chin. Phys.* **14** 2269
[36] Vast V, Baroni S, Zerah G, Besson J M, Polian A, Grimsditch M and Chervin J C 1997 *Phys. Rev. Lett.* **78** 693
[37] Werheit H , Rotter H W, Meyer F D, Hillebrecht H, Shalamberidze S O, Abzianidze T G and Esadze G G 2004 *J. Solid State Chem.* **177** 569
[38] Werninghaus T, Hahn J Richter F and Zahn D R T 1997 *Appl. Phys. Lett.* **70** 958
[39] Werheit H, Boron Compounds, in : O. Madelung (Ed.), Landolt-Börnstein, 2000 New Series Group III **41D** (Berlin: Springer) pp1–492
[40] Schmechel R, Werheit H, Kampen T U and Mönch W 2004 *J. Solid State Chem.* **177** 566
[41] Werheit H, Binnebruck H and Hausen A 1971 *Phys. Stat. Sol* (b) **47** 63
[42] Choi H J, Johnson J J, He R, Lee S K, Kim F, Pauzaauski P, Goldgerger J, Saykally R J and Yang P 2003 *J. Phys. Chem.* B **107** 8721
[43] Wang X J, Tian J F, Bao L H, Hui C, Yang T Z, Liu F, Xu N S, Shen C M and Gao H J 2007 *J. Appl. Phys.* **102** 0143091